



COHERENT MOTIONS AND CLUSTERS IN A DISSIPATIVE MORSE RING CHAIN

J. DUNKEL*, W. EBELING and U. ERDMANN

*Institute of Physics, Humboldt University,
Invalidenstraße 110, D-10115 Berlin, Germany*

**University of Oxford, Exeter College, OX1 3DP Oxford, UK
dunkel@physik.hu-berlin.de*

V. A. MAKAROV

*Instituto Pluridisciplinar, Universidad Complutense,
Paseo Juan XIII, 1, 28040 Madrid, Spain*

Received April 4, 2001; Revised November 30, 2001

We study a one-dimensional ring chain of length L with N particles interacting via Morse potentials and influenced by dissipative forces (passive and active friction). We show that by negative friction the system can be driven far from the thermodynamic equilibrium states. For over-critical pumping with free energy several types of coherent motions including uniform rotations, optical oscillations and waves emerge in the ring. We also show the existence of a critical particle density $n_c = N/L_c$, below that the particles spontaneously organize into clusters which can actively rotate. Additionally, the influence of white noise on the clustering is discussed.

Keywords: Nonlinear friction; active Brownian particles; Lennard–Jones-like interactions; cluster formation.

1. Introduction

After pioneering work by Toda [1983] who analytically proved the existence of solitons in a special Hamiltonian lattice system, the excitations in a dissipative Toda chain were studied mainly for the case of passive friction or embedding into a heat bath [Bolterauer & Oppen, 1981; Toda & Saitoh, 1983; Ebeling & Jentsen, 1991; Jentsen & Ebeling, 2000]. Recently a concept of dissipative solitons propagating in systems with energy supply has attracted great interest [Chu & Velarde, 1991; Christov & Velarde, 1995]. In our previous work we have studied dissipative lattices with Toda interactions and have shown [Makarov *et al.*, 2000; Ebeling *et al.*, 2000] that dissipative solitons can emerge in these systems due to appropriate energy-dissipation

balance. The Toda potential is given by

$$U_i^T = \frac{a}{b}(e^{-br_i} - 1) + ar_i \quad (1)$$

and it is closely related to the exponential potential

$$U_i^E = \frac{a}{b}e^{-br_i}. \quad (2)$$

One of the reasons for the special interest in Toda systems is the existence of exact solutions in the Hamiltonian case and for the statistical thermodynamics [Toda, 1983; Toda & Saitoh, 1983]. On this basis it has been shown e.g. in [Bolterauer & Oppen, 1981; Jentsen & Ebeling, 2000] that phonon excitations dominate the spectrum at low temperatures and strongly localized soliton excitations are the most relevant at high temperatures. Here we

shall concentrate on a Morse lattice with dissipative, velocity-dependent friction interacting with a heat bath modeled by white noise. We differ between passive friction where the friction coefficient $\gamma(v)$ is strictly positive and active friction when $\gamma(v)$ also contains a negative part corresponding to pumping of free energy into the system [Rayleigh, 1945; Schweitzer *et al.*, 1998; Ebeling *et al.*, 1999; Erdmann *et al.*, 2000].

The Morse potential (Fig. 1) is a combination of two exponential interactions with different signs [Ebeling *et al.*, 1989] and is defined by

$$U_i^M = \frac{a}{2b}[e^{-2br_i} - 2e^{-br_i}] = \frac{a}{2b}(e^{-br_i} - 1)^2 - \frac{a}{2b}. \quad (3)$$

For all potentials (1)–(3) the parameters b and a control the stiffness of the spring connecting two interacting particles and the amplitude of the corresponding force. The coordinates

$$r_i = x_{i+1} - x_i - \sigma \quad (4)$$

represent the distance between two neighboring particles located at positions x_{i+1} and x_i reduced by the equilibrium length of the springs, σ . In this notation Morse and Toda potentials have their minimum at $r_i = 0$. For small deviations from the minimum we obtain the frequency of harmonic oscillations, ω_0 , which is the same for U_i^T and U_i^M

$$\omega_0^2 = \frac{ab}{m} \quad (5)$$

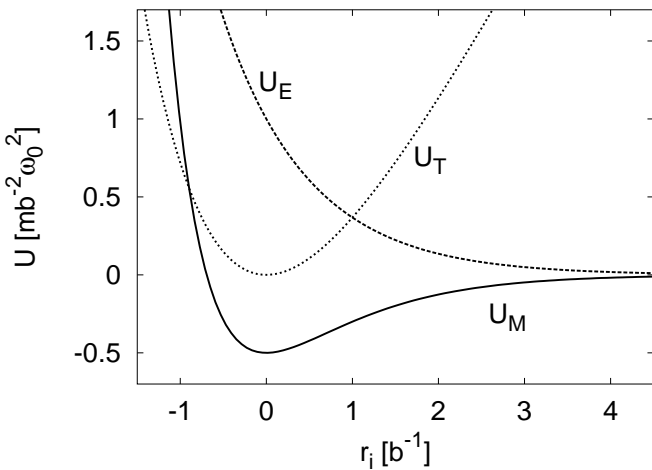


Fig. 1. Shapes of Morse, U_M , Toda, U_T , and exponential, U_E , potentials ($a = 1$, $b = 1$ and $\sigma = 1$; units are $[a] = m\omega_0^2/b$, $[\sigma] = b^{-1}$).

where m is the mass of the particles. Morse and Toda potentials possess an attracting part, whereas the force derived from the exponential potential (2) is purely repulsive. Nevertheless, exponential and Toda potentials lead to equivalent dynamical systems since in both cases the effective potential describing the motion of the i th particle

$$U_i^{\text{eff}}(x_i, x_{i-1}, x_{i+1}) = U_{i-1}(r_{i-1}) + U_i(r_i) \quad (6)$$

has equivalent cosh-shape. In contrast, for Morse interaction the shape of the effective potentials depends on the distances between the particles

$$d_{i+1,i-1} = x_{i+1} - x_{i-1} = r_i + r_{i-1} + 2\sigma$$

i.e. on the local particle density. Namely, the shape can change from mono-stable to bistable (Fig. 2). As we shall see further this leads to basically new effects e.g. the formation of clusters of particles. If the springs' stiffness, b , is very small the effective potentials U_i^{eff} for a Toda ring is almost harmonic and for large b it becomes similar to hard-core potentials. The main difference between Toda and Morse interactions is their behavior for long distances between the particles. Only for Morse interaction the forces tend to zero for $r_i \rightarrow \infty$. As can be seen in Fig. 1 the Morse potential is qualitatively similar to the LJ-potential that is used to describe real molecular interactions. Compared to the Toda potential the Morse potential is more realistic, but there are not many exact analytical results for a Morse chain.

Results of recent investigations concerning active Toda rings can be found in [Makarov *et al.*,

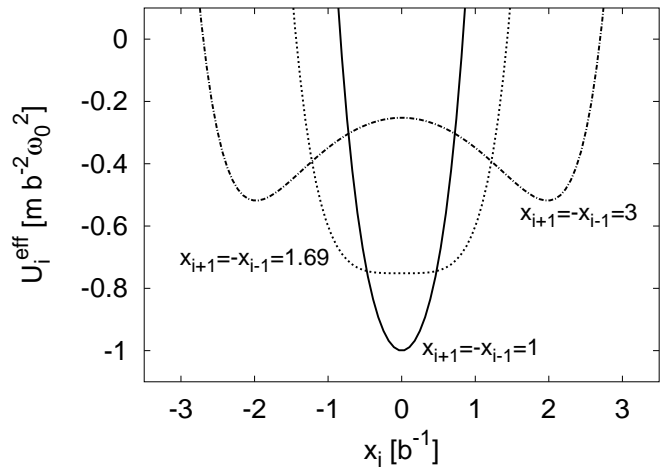


Fig. 2. Shapes of effective Morse potential U_i^{eff} for different distances between particles ($a = 1$, $b = 1$ and $\sigma = 1$). The effective potential is bistable for $d_{i+1,i-1} > 2(\sigma + b^{-1} \ln 2)$ and mono-stable otherwise.

2000; Ebeling *et al.*, 2000; Makarov *et al.*, 2001]. There it has been shown theoretically, numerically and experimentally that for different types of active friction stable running solitons and soliton-like excitations can be generated in a Toda ring. Makarov *et al.* [2001] tested their theoretical predictions experimentally using an analog electrical circuit and found a good agreement between theory and experiment. As indicated above a Toda ring effectively obeys the same dynamical equations like a ring with purely repulsive exponential interactions and for high particle densities the dynamics of a Morse ring is also very similar. The essential difference in dynamics of Morse and Toda lattices appears at low particle densities.

The paper is organized as follows. In Sec. 2 we discuss dissipative forces acting on the particles and introduce the equations of motions. Section 3 is devoted to the investigation of the dynamics of a deterministic Morse ring with passive forces and to comparing the results to the Toda case. We shall show that clustering processes in a Morse ring strongly depend on the relation of the average distance between the masses, $l = L/N$, and the equilibrium length of the Morse springs, σ . Clustering may be observed if $l \gg \sigma$, i.e. for the low enough mean particle density, $n = N/L$. In the opposite case of high densities the particles mainly feel the exponential repulsion and therefore behave very similar to the Toda case. In Sec. 4 we investigate the active Morse ring and discuss the appearance of oscillatory and wavy motions that can be observed inside clusters. In Sec. 5 we study the influence of noise on the clustering processes and give a simple phase transition like diagram. Finally, in Sec. 6 we summarize our results.

2. Dissipative Forces and Motion Equations

Let us consider a one-dimensional model of active Brownian particles consisting of N point masses m located at the coordinates x_i ($i = 1, \dots, N$) on a ring of length L . The mean distance between particles, l , and the particle density, n , are

$$l = n^{-1} = \frac{L}{N}. \quad (7)$$

The particles are connected to their next neighbors

at both sides by pair interaction forces

$$F_i = F(x_{i-1}, x_i, x_{i+1}) = -\frac{\partial U_i^{\text{eff}}}{\partial x_i}. \quad (8)$$

The periodic boundary conditions assume

$$x_{i+N} = x_i + L. \quad (9)$$

We shall discuss the dynamics of a homogeneous finite size Morse ring with particles influenced by a velocity dependent friction forces $\Gamma(v_i)$ and later we shall also include the effects of a coupling of the system to a heat bath modeled by additive Gaussian white noise. With regard to all influences the dynamics of our Brownian particles is determined by the following Langevin equations

$$\frac{dx_i}{dt} = v_i, \quad m \frac{dv_i}{dt} - F_i = \Gamma(v_i) + m\sqrt{2D}\zeta_i(t). \quad (10)$$

The white noise on the r.h.s. of (10) is characterized by

$$\langle \zeta_i(t) \rangle = 0 \quad \langle \zeta_i(t) \zeta_j(t') \rangle = \delta_{ij} \delta(t - t').$$

The constant D controls the intensity of the stochastic forces representing the interactions between Brownian particles and surrounding heat bath (e.g. smaller molecules). The deterministic dissipative force in (10) is given by $\Gamma(v_i) = -\gamma(v_i^2)v_i$. As a simple model we consider the active friction function earlier proposed in [Schweitzer *et al.*, 1998; Ebeling *et al.*, 1999]

$$\gamma(v^2) = \gamma_0 - \frac{d_2 q}{c + d_2 v^2} = \gamma_0 - \frac{q}{\frac{c}{d_2} + v^2}. \quad (11)$$

In this model active particles are characterized by internal energy depots and internal dissipation [Schweitzer *et al.*, 1998; Ebeling *et al.*, 1999]. The parameter γ_0 is the usual viscous friction parameter, while q describes the flux of energy from an external reservoir or field into the particles. The parameter c is connected to internal dissipation and d_2 controls the conversion of the energy received from the field into kinetic energy (according to the r.h.s. of (11) their ratio c/d_2 is important). In case of no feeding with energy ($q = 0$) or no energy conversion ($d_2 = 0$) the friction is purely passive. It is useful to rewrite the friction term (11) in the form

$$\gamma(v^2) = \gamma_0 d_2 \frac{v^2 - \mu}{c + d_2 v^2} \quad (12)$$

with

$$\mu = \frac{q}{\gamma_0} - \frac{c}{d_2}. \tag{13}$$

Here μ plays the role of a bifurcation parameter. Since $\gamma(v^2) = 0$ for $v = \pm\sqrt{\mu}$, a single pumped particle aims to reach one of these velocities in the stationary state (corresponding to clockwise/counterclockwise rotations on the ring). This corresponds to so-called active motions. Parameter values $\mu < 0$ lead to a damped system. For negative μ the only stationary stable velocity is $v = 0$, i.e. all motions decay to the rest after a relaxation time. For $\mu > 0$ the friction term $\gamma(v^2)$ converges to γ_0 at large velocities while for small velocities $v^2 < \mu$ the friction function is negative. This region corresponds to a pumping with free energy at the cost of the external reservoir and the dynamics develops active forms of motions. Thus a system with a single particle undergoes a pitchfork-bifurcation [Wiggins, 1996] at $\mu = 0$. We shall see below that near $(v, \mu) = (0, 0)$ the active friction introduced in (11) is similar to the well-known Rayleigh model [Rayleigh, 1945]

$$\gamma(v^2) = \gamma_0(v^2 - \mu). \tag{14}$$

For $v^2 \gg \mu$ both models behave differently. In this limit the Rayleigh-model diverges, while the depot model converges to the passive (viscous) friction.

Notes on units. Before we continue with the discussion of the equations of motions it is useful to reduce the number of parameters in our model by choosing appropriate units of reference. Since the ring is homogeneous we define m as unit mass, b^{-1} as unit length and ω_0^{-1} as unit time. Then we may simply set $m = 1$, $b = 1$ and $\omega_0 = 1$ whenever they appear in the equations of motions. This procedure automatically implies that all parameters are given in these units as well (e.g. $[\gamma_0] = m\omega_0$, $[U_i] = mb^{-2}\omega_0^2$, etc.) and with respect to (5) we also have $a = 1$. Besides, we fix $c/d_2 = 1$ throughout the whole paper i.e. the energy conversion rate of particles is equal to the internal dissipation rate. This choice of parameters has no qualitative consequences on the dynamics, but the variation of the parameter μ is now exclusively connected to variations of the ratio q/γ_0 . With these conventions we can rewrite Morse (3) and Toda potential (1)

$$\begin{aligned} U_i^M &= \frac{1}{2}(e^{-r_i} - 1)^2 - \frac{1}{2} \\ U_i^T &= e^{-r_i} - 1 + r_i, \end{aligned} \tag{15}$$

the friction coefficient (12)

$$\gamma(v^2) = \gamma_0 \frac{v^2 - \mu}{1 + v^2} \tag{16}$$

and the Langevin equations (10)

$$\frac{dx_i}{dt} = v_i, \quad \frac{dv_i}{dt} - F_i = -\gamma(v_i^2)v_i + \sqrt{2D}\zeta_i(t). \tag{17}$$

where v_i is the velocity of the i th particle that is now equivalent to its momentum in the chosen units.

3. Deterministic Morse Ring with Passive Damping Forces

Let us start with noise free (deterministic) system by setting $D = 0$ in (17). Besides we assume that the friction is purely passive i.e. $\mu < 0$ ($\gamma(v^2) > 0$). In the units chosen above, the Hamiltonian of the conservative ring is

$$H = \sum_{i=1}^N \left[\frac{v_i^2}{2} + U_i \right]. \tag{18}$$

where potential energy U_i is defined by (15). For the dissipative system with $\mu < 0$ its full energy decays in time

$$\frac{dH}{dt} = - \sum \gamma(v_i^2)v_i^2 \leq 0. \tag{19}$$

Thus a minimum of the potential energy is finally approached. Further, besides linear coordinates, x_i , we shall use $N - 1$ relative coordinates, r_i , (4) and the coordinate of the ‘‘center of mass’’, s ,

$$s = \frac{1}{N} \sum_{i=1}^N x_i. \tag{20}$$

The N th relative coordinate follows automatically from the others because of the constant ring length L . The relative coordinates, r_i , obey the condition

$$\frac{1}{N} \sum_{i=1}^N r_i = l - \sigma \tag{21}$$

where $(l - \sigma)$ is the mean elongation of the springs due to the possible mismatch between the ring length, $L = Nl$, and the sum of the equilibrium lengths of springs given by $N\sigma$. Obviously the full potential energy $U = \sum_i U_i$ of the ring does not depend on s but only on the relative coordinates r_i . In

the case of constant dissipative force ($\gamma(v^2) = \gamma_0$) the equations of motion for a Toda ring are

$$\begin{aligned} \ddot{r}_i + \gamma_0 \dot{r}_i &= 2e^{-r_i} - e^{-r_{i+1}} - e^{-r_{i-1}} \equiv f^T(r_j) \\ \ddot{s} + \gamma_0 \dot{s} &= 0. \end{aligned} \quad (22)$$

For $\gamma_0 = 0$ the system (22) is of Hamiltonian type and as we know from Toda's theory [Toda, 1983; Landa, 1996] it possesses analytical solutions e.g. soliton solutions. For passive dissipative forces $\gamma(v^2) > 0$ the attractors of the system are given by the minima of the potential energy U since the full energy decays in time (19). For a Morse ring we find the similarly looking dynamical equations

$$\begin{aligned} \ddot{r}_i + \gamma_0 \dot{r}_i &= (2e^{-2r_i} - e^{-2r_{i+1}} - e^{-2r_{i-1}}) \\ &\quad - (2e^{-r_i} - e^{-r_{i+1}} - e^{-r_{i-1}}) \\ &= f^T(2r_j) - f^T(r_j) \equiv f^M(r_j) \\ \ddot{s} + \gamma_0 \dot{s} &= 0. \end{aligned} \quad (23)$$

In the high particle density limit ($l \ll \sigma$) the relative coordinates satisfy the condition $r_i \ll 0$. Hence, we get asymptotically $f^M(r_j) \rightarrow f^T(2r_j)$ and find in the Morse chain Toda-like solutions with stiffness $2b$ for high particle densities.

In order to study the steady states of the effectively damped systems with $\mu < 0$ we begin with an investigation of the full potential energy in Toda and Morse rings. In case of a Toda ring the full potential energy $U^T = \sum_i U_i^T$ has a single (global) minimum at $r_i = l - \sigma$ corresponding to an equidistant distribution of all particles on the ring. This property is valid for any parameter values. Thus independent of the initial conditions and parameter values the equidistant stationary distribution is realized in the damped Toda ring. For $l < \sigma$ ($l > \sigma$) all springs in the stationary state are compressed (decompressed) with regard to their equilibrium length, σ . Now let us look at the ring with the Morse potential given by (15). Similar to the Toda potential the Morse potential is repulsive for $r_i < 0$ and attractive for $r_i > 0$ but in contrast to U_i^T the Morse potential converges to zero for $r_i \rightarrow \infty$. The main consequence is that the effective potentials become bistable (Fig. 2) if the mean distance between the particles, l , is large enough. Hence the equilibrium states now depend on the mean particle density $n = l^{-1}$ and the equilibrium spring length σ . To describe the physics of the Morse ring that is in parts known from equilibrium statistical mechanics of the one-dimensional gas [Kac *et al.*, 1963;

Feynman, 1972; Percus, 1987] we study the minima of the full potential energy given by

$$U^M(r_1, \dots, r_N) = \frac{1}{2} \sum_{i=1}^N [(e^{-r_i} - 1)^2 - 1]. \quad (24)$$

Introducing $X_i = e^{-r_i}$, $\Lambda = e^{-N(l-\sigma)}$ and using (21) we can rewrite (24)

$$\begin{aligned} U^M(r_1, \dots, r_N) &= U^M(X_1, \dots, X_{N-1}) \\ &= \frac{1}{2} \left[\left(\frac{\Lambda}{\prod_{j=1}^{N-1} X_j} - 1 \right)^2 - N + \sum_{i=1}^{N-1} (X_i - 1)^2 \right]. \end{aligned} \quad (25)$$

Studying the minima of the potential energy U^M we find that the equidistant distribution $r_i = l - \sigma$ or $X_i = \Lambda^{1/N}$ corresponds to a minimum only as long as the particle density is higher than a critical value i.e.

$$n = l^{-1} > n_c = \frac{1}{\ln 2 + \sigma}. \quad (26)$$

This property of the Morse ring can be obtained from an analysis of the Hessian matrix $\mathcal{H}[U^M]$. In the density region $n \gg n_c$ Morse and Toda rings show qualitatively the same mono-stable behavior. For low particle density, $n < n_c$, the equidistant distribution, $r_i = l - \sigma$, corresponds to a local maximum of U^M , hence is unstable. In this situation we always have N equivalent global minima each corresponding to the configuration where all particles form one big cluster of size N , i.e. each particle is located in a minimum of the bistable effective potentials caused by its neighbors. If we imagine that there are N possibilities to fill the first place in the cluster it becomes clear that we have N such minima. The important question is: At which densities $\bar{n}_c = \bar{n}_c(N)$ do these new minima appear for the first time? To answer this question let us consider several simple cases.

For $N = 2$ the potential energy (25) depends on one independent coordinate, X_1 , only and has minima at

$$X_1 = \begin{cases} \sqrt{\Lambda} & \Lambda \in \left(\frac{1}{4}, \infty \right) \\ \frac{1}{2} \pm \frac{1}{2} \sqrt{1 - 4\Lambda} & \Lambda \in \left(0, \frac{1}{4} \right) \end{cases} \quad (27)$$

The first solution (one minimum) corresponds to the equidistant distribution already described above

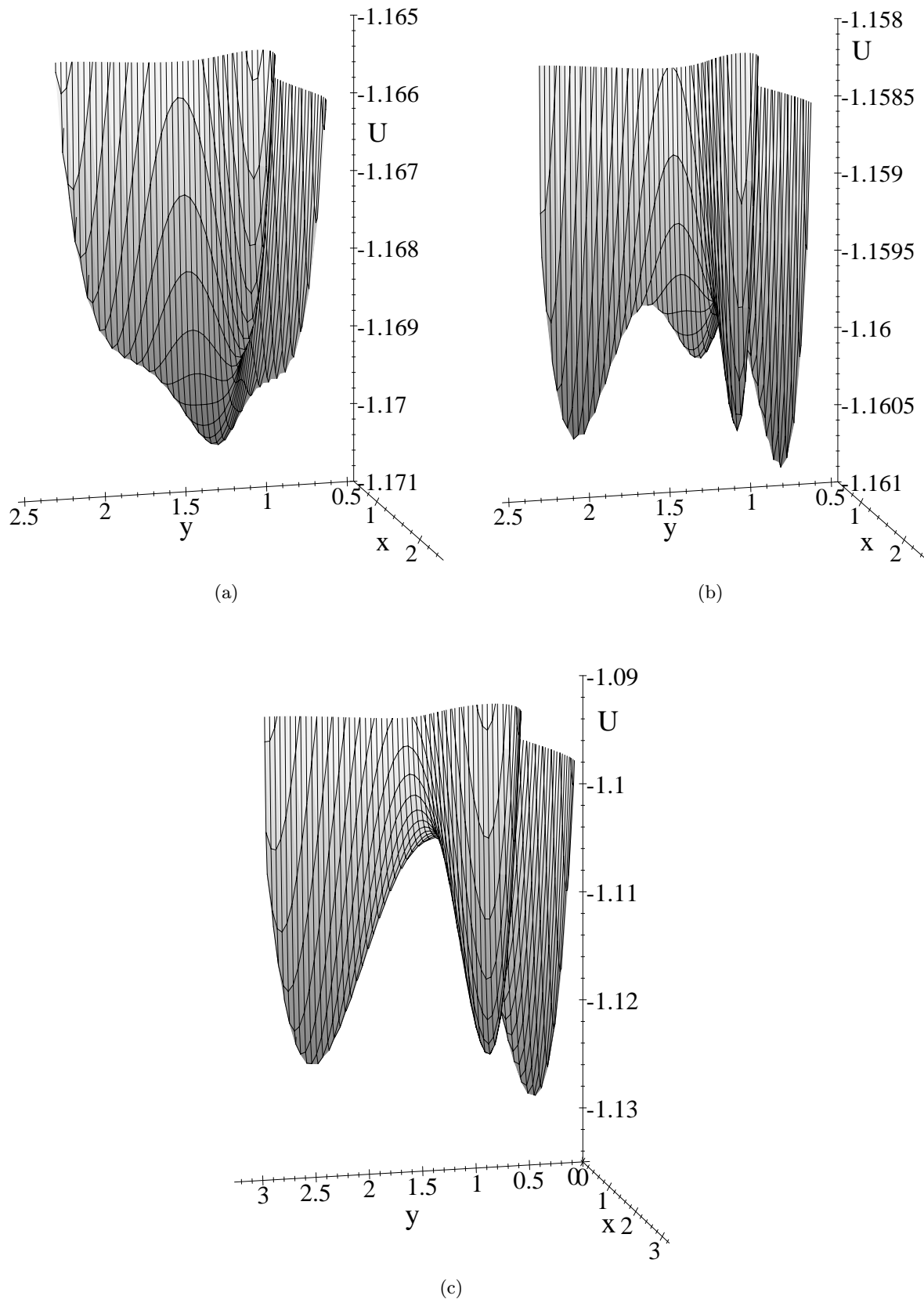


Fig. 3. Potential energy of the Morse ring with three particles and $\sigma = 1$ leading to $n_c = 0.591$ and $\bar{n}_c = 0.611$. The x -axis corresponds to the distance between particles 1 and 2 and the y -axis to the distance between particles 2 and 3. (a) Mono-stable region $n = 0.612 > \bar{n}_c$. (b) Transition region $\bar{n}_c > n = 0.607 > n_c$. (c) Pure clustering region $n_c > n = 0.579$. The units are $[U] = mb^{-2}\omega_0^2$, $[x] = [y] = b^{-1}$ and $[n] = b$.

and the second one (two minima) to clusters. Thus we have one bifurcation at $\Lambda = 1/4$ and hence two critical values of the particle density are the same, $\bar{n}_c = n_c$. Considering this bifurcation at the critical density n_c (26) we introduce in addition to μ a second bifurcation parameter

$$\alpha = l - (\sigma + \ln 2). \quad (28)$$

Hence, the parameter α accounts for the deviation of the mean particle distance, l , from its critical value. Values $\alpha < 0$ ($\alpha > 0$) correspond to mono-stable (bistable) potential energy U^M .

For the more complicated case of three particles, $N = 3$, the potential energy depends on two variables X_1 and X_2 . Here we find that U^M has minima at

$$(X_1, X_2) = \begin{cases} (\Lambda^{\frac{1}{3}}, \Lambda^{\frac{1}{3}}) & \Lambda \in \left(\frac{1}{8}, \infty\right) \\ (Z_0, Z_0) & \Lambda \in \left(0, \frac{4}{27}\right) \\ (1 - Z_0, Z_0) & \Lambda \in \left(0, \frac{4}{27}\right) \\ (Z_0, 1 - Z_0) & \Lambda \in \left(0, \frac{4}{27}\right) \end{cases} \quad (29)$$

where $Z_0 > 0$ is the solution of $f(Z) \equiv Z^3 - Z^2 + \Lambda = 0$. The first solution again corresponds to equal distances between the particles and the Λ -interval follows from (26). The other three solutions represent the three stationary cluster configurations. Here the condition for Λ may be obtained in the following way: $f(Z)$ has the only local minimum $f(2/3) = \Lambda - (4/27)$ and the only local maximum $f(0) = \Lambda$. Thus $f(Z) = 0$ has a positive solution only if $\Lambda < 4/27$ (note that $\Lambda > 0$, $X_i > 0$ due to their definition). From the critical value $\Lambda = 4/27$ we obtain

$$\bar{n}_c(3) = \frac{3}{\ln \frac{27}{4} + 3\sigma} > n_c \Leftrightarrow l < \sigma + \ln \left(\frac{27}{4}\right)^{\frac{1}{3}}. \quad (30)$$

This means that there is a transition interval (n_c, \bar{n}_c) where both cluster and equidistant stable configurations coexist. Figure 3 shows three plots of U^M for the different density regions. The procedure applied for $N = 3$ can be similarly used for $N > 3$. The calculations are more difficult but the results are qualitatively the same. The transition interval

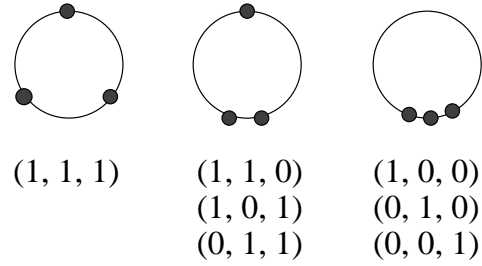


Fig. 4. Sketch diagrams of stable and unstable configurations in the Morse ring with three particles ($\alpha > 0$ and $\mu < 0$). The equidistant configuration $(1, 1, 1)$ corresponds to a local maximum of the potential energy and becomes a minimum for $n > n_c$ ($\alpha < 0$). The second ring corresponds to the saddle points of the potential energy (see also Fig. 3). The third ring represents the minima (clusters) existing for $n < \bar{n}_c$.

(n_c, \bar{n}_c) becomes larger with increasing N but is obviously bounded by the condition $\bar{n}_c < \sigma^{-1}$.

In addition to the extrema for $n < n_c$ there appear many saddle points in the global potential energy landscape. These metastable points correspond to symmetric combinations of smaller clusters. In order to count the number of all equilibria (minima, maxima and saddles) for a ring with N particles and $n < n_c$ we introduce binary vectors of length N excluding $(0, 0, \dots, 0)$. That means we assign 1 to particle i if it is the first particle in a cluster and 0 otherwise. For example, the vector $(1, 0, \dots, 0)$ corresponds to the global minimum with the first particle at the beginning of the N -cluster and $(1, 1, \dots, 1)$ to the local maximum corresponding to equal distances between all particles. Then the total number of equilibria is $W_N = 2^N - 1$ and the number of saddle-points is $W_N^{\text{sp}} = 2^N - 2 - N$. Figure 4 shows the configurations corresponding to the maximum, minima and saddles in case $N = 3$ and $n < n_c$. In the case of effectively passive friction $\mu < 0$ the ring will relax into one of the minima of the potential energy.

4. Deterministic Morse Ring with Active Friction

Deterministic dissipative Toda chains with energy supply have been studied in several recent papers e.g. with the aim to model stationary solitons [Ebeling *et al.*, 2000; Makarov *et al.*, 2000; Makarov *et al.*, 2001]. Makarov *et al.* [2001] gave an extensive discussion of an active Toda chain with Rayleigh-type friction and Ebeling *et al.* [2000] investigated the behavior of a Toda chain in the limit of large

parameter values b using the friction function introduced in (13). Before discussing an active Morse ring characterized by $\mu > 0$ we shall summarize the results already known for active Toda chains. For a Toda ring with N particles driven by depot energy there exist $N + 1$ qualitatively different attractors which could be identified as two stationary uniform rotations $(\dot{s}, r_i) = (\pm\sqrt{\mu}, l - \sigma)$ and $N - 1$ oscillatory modes (corresponding to one-soliton-solutions, two-soliton-solutions, etc. and finally stationary, optical oscillations if $N = \text{even}$). Each attractor has a symmetric partner (e.g. left-handed and right-handed rotations). Compared with a Toda system we find nearly the same behavior for a Morse ring with high densities $n > \bar{n}_c$. Qualitatively new results can be expected in the Morse ring chain if $n < \bar{n}_c$, i.e. at low particle densities. Thus in contrast to previous investigations of a Toda ring which concentrated on the existence of stable waves we will now also look for active motions of or within clusters. In order to understand the new effects we begin our studies of an active Morse ring with the first nontrivial case $N = 2$ which is already very suitable to point out the parallels and differences in the dynamics of active Toda and Morse rings.

4.1. Morse ring with two particles

For a ring with $N = 2$ effective and full potential energies are equivalent. In this case we are able to carry out a complete analysis of the phase space of the system. We shall study on bifurcations in the parameter space (μ, α) . For simplification we also set the viscous friction parameter $\gamma_0 = 1$ whenever dealing with an active ring. Then a variation of the bifurcation parameter μ is equivalent to a change of the energy uptake rate q . For convenience we introduce the following coordinates

$$\begin{aligned} y &= x_2 - x_1 - L/2 & p_y &= v_2 - v_1 \\ z &= x_1 + x_2 & p_z &= v_1 + v_2. \end{aligned} \tag{31}$$

The coordinate y plays the role of a relative coordinate and z may be interpreted as ‘‘center of mass’’ coordinate. Then we can rewrite the equations of motions for active Morse ring with two particles in the form

$$\begin{aligned} \dot{y} &= p_y \\ \dot{z} &= p_z \\ \dot{p}_y &= 4A \sinh(y) - 4A^2 \sinh(2y) + \Gamma_y(p_y, p_z) \\ \dot{p}_z &= \Gamma_z(p_y, p_z) \end{aligned} \tag{32}$$

where

$$\begin{aligned} \Gamma_y(p_y, p_z) &= \Gamma\left(\frac{p_z + p_y}{2}\right) - \Gamma\left(\frac{p_z - p_y}{2}\right) \\ \Gamma_z(p_y, p_z) &= \Gamma\left(\frac{p_z + p_y}{2}\right) + \Gamma\left(\frac{p_z - p_y}{2}\right) \end{aligned} \tag{33}$$

and

$$A = \frac{1}{2}e^{-\alpha}. \tag{34}$$

In this notation the critical value $\alpha = 0$ corresponds to $A = 1/2$ and $\alpha > 0$ ($\alpha < 0$) to $A < 1/2$ ($A > 1/2$). The dynamical system (32) is invariant under the transformation $(y, z, p_y, p_z, t) \rightarrow (-y, -z, -p_y, -p_z, t)$. Time reversal is excluded because of the dissipative terms. The z coordinate has no influence on the dynamical flow so the system (32) can be effectively reduced to the system for (y, p_y, p_z) . We immediately see, that all fixed points are situated in the $(p_y = 0)$ -plane of the reduced $3d$ -phase space. We now discuss the steady states for different signs of the bifurcation parameters μ and α . In order to give a complete discussion for a Morse ring with two particles at this point we shall include some short remarks concerning the damping case $\mu < 0$ in spite of the fact that it is already covered by the discussion in Sec. 3.

4.1.1. Steady states and their bifurcations

In the parameter region $\mu < 0, \alpha < 0$ the reduced system (32) has only one attractor (due to (19) and mono-stability of the effective potential), which is given by the globally stable steady state in the origin $S_0 = (0, 0, 0)$ with eigenvalues

$$\lambda_1 = \mu, \quad \lambda_{2,3} = \frac{1}{2}(\mu \pm \sqrt{\mu^2 + 16A - 32A^2}).$$

Now let us consider bifurcations of this steady state (that exists for all parameter values) when parameters μ and α are changed. When α passes through zero to the domain $\mu < 0, \alpha > 0$ the system (32) undergoes a pitchfork bifurcation. Two new stable steady states $S_{1,2} = (y_{1,2}, 0, 0)$ appear, while S_0 becomes a saddle. This corresponds to the bistable interaction potential with minima at

$$y_{1,2} = \pm \cosh^{-1}\left(\frac{1}{2A}\right). \tag{35}$$

The new stable steady states $S_{1,2}$ have the following eigenvalues

$$\lambda_1 = \mu, \quad \lambda_{2,3} = \frac{1}{2}(\mu \pm \sqrt{\mu^2 - 8 + 32A^2}),$$

and correspond to cluster configurations of the particles in the ring. Now let us come back to the steady state S_0 and parameter domain $\mu < 0, \alpha < 0$. Increasing μ , again at $\mu = 0$ we get a pitchfork bifurcation. In the domain $\mu > 0, \alpha < 0$ corresponding to over-critical pumping and mono-stability of the effective Morse potential a new pair of symmetric stable steady states $S_{3,4} = (0, 0, \pm 2\sqrt{\mu})$ appears. Their eigenvalues are

$$\lambda_1 = -\frac{2\mu}{1 + \mu},$$

$$\lambda_{2,3} = -\frac{\mu \pm \sqrt{\mu^2 + (4A - 8A^2)(1 + \mu)^2}}{1 + \mu}.$$

These steady states correspond to constant rotations of the particles with equal distances, $L/2$, between them. Besides the pitchfork bifurcation, on the line $\mu = 0$ a Hopf bifurcation occurs. The steady state in the origin, S_0 , becomes unstable and a limit cycle is born. As we shall see further this limit cycle is stable. It corresponds to so-called “optical” oscillations, when particles oscillate in anti-phase. Similar bifurcations occur with the steady states $S_{1,2}$ ($\alpha > 0$), when μ passes zero. New stable steady states $S_{5-8} = (y_{1,2}, 0, \pm 2\sqrt{\mu})$ appear in the region $\mu > 0, \alpha > 0$. Their eigenvalues are

$$\lambda_1 = -\frac{2\mu}{1 + \mu},$$

$$\lambda_{2,3} = -\frac{\mu \pm \sqrt{\mu^2 + 2(4A^2 - 1)(1 + \mu)^2}}{1 + \mu}.$$

Additionally, two limit cycles are born at $\mu = 0$ via Hopf bifurcations. The steady states S_{0-4} are all unstable in this domain which corresponds to an active Morse ring with bistable potential. The steady states S_{5-8} correspond to left/right-rotations of two-particle-clusters and limit cycles describe optical oscillations of particles grouped in a cluster.

Thus we have found two bifurcation lines for steady states: (i) $\alpha = 0$ with pitchfork bifurcation and (ii) $\mu = 0$ with pitchfork and Hopf bifurcations.

4.1.2. Periodic orbits

As we have seen above, depending on α one or two limit cycles appear via Hopf bifurcation when μ

passes zero to positive values. These limit cycles lie within the invariant manifold ($p_z = 0$) of the dynamical system (32). Let us start with an investigation of the dynamics for small positive μ . In the mono-stable region $\alpha < 0 \Leftrightarrow A > 1/2$ we can write $A = (1/2) + \delta$. Changing coordinates $y = \beta u, p_y = \sqrt{\beta}v, p_z = \sqrt{\beta}w$ and $\tau = t/\sqrt{\beta}$ with $\beta = 4\delta(1 + 2\delta)$ and expanding \sinh and $\Gamma_{y/z}$ in (32) for small amplitudes (requires $\mu \ll 1$) we obtain

$$\begin{aligned} \dot{u} &= v \\ \dot{v} &= -u + \varepsilon \left\{ v[16(1 + 2\delta)\mu - v^2 - 3w^2] \right. \\ &\quad \left. - \frac{3 + 8\delta}{6\delta\sqrt{\delta + 2\delta^2}} u^3 \right\} \\ \dot{w} &= \varepsilon w[16(1 + 2\delta)\mu - 3w^2 - v^2] \end{aligned} \tag{36}$$

where $\varepsilon = (1/32)(\delta + 2\delta^2)^{-(3/2)}$ is a small parameter and $\dot{u} = du/d\tau$. The approximation of the system (32) by the perturbed harmonic system (36) is valid as long as $\delta \gg 0.2$ and $\mu \ll 32\sqrt{\delta}$ because under these conditions the perturbation becomes sufficiently small. We can see that in the case of $w = 0$ (or $v = 0$) the dissipative terms in (36) are of Rayleigh-type. Using cylindrical coordinates (a, θ, w) with $(u, v) = (a \cos \theta, -a \sin \theta)$ and $\theta = \phi + \tau$ (where $a = a(\tau)$ and $\phi = \phi(\tau)$ are slow functions of τ) we can apply the method of averaging [Guckenheimer & Holmes, 1983] and get

$$\begin{aligned} \dot{a} &= -\varepsilon \frac{a}{8} \{ 3a^2 + 4[3w^2 - 16(1 + 2\delta)\mu] \} \\ \dot{w} &= -\varepsilon \frac{w}{2} \{ 3a^2 + 2[w^2 - 16(1 + 2\delta)\mu] \} \\ \dot{\phi} &= \varepsilon \frac{a^2(3 + 8\delta)}{16\delta\sqrt{\delta + 2\delta^2}}. \end{aligned} \tag{37}$$

Now we can follow the proof given in [Makarov *et al.*, 2001]. In the averaged system (37) the first two equations do not depend on ϕ so we can consider them separately from the third one. Additionally the system (37) is symmetric with regard to the transformation $a \rightarrow -a$ and (or) $w \rightarrow -w$ so we can restrict our investigations to the first quadrant of the (a, w) -plane. There we find four steady states $P_{1-4} = \bar{P}_{1-4}\sqrt{\mu(\delta + 2\delta^2)}$ with

$$\begin{aligned} \bar{P}_1 &= (\bar{a}_1, \bar{w}_1) = (0, 0) & \bar{P}_2 &= \left(\sqrt{\frac{128}{15}}, \frac{4}{\sqrt{5}} \right) \\ \bar{P}_3 &= \left(\frac{8}{\sqrt{3}}, 0 \right) & \bar{P}_4 &= (0, 4). \end{aligned} \tag{38}$$

P_1 is unstable, P_2 is a saddle and $P_{3/4}$ are stable. The fixed point P_4 corresponds to $\dot{\phi} = 0$ and describes the rotation of the particles already found. The third steady state, P_3 , corresponds to a stable limit cycle in the integral surface $w = 0 \Leftrightarrow p_z = 0$. Moreover it was shown in [Makarov et al., 2001] that systems like (36) do not have any other attractors. In the mentioned work the existence of a globally attracting domain bounded by two elliptical curves in the (a, w) -plane has been proven. Then it has been shown that this domain does not contain other attractors rather than P_2 and $P_{3/4}$ by using Bendixon’s criterion [Guckenheimer & Holmes, 1983]. Inverting the transformations we obtain the (dimensionless) oscillation amplitudes and frequency

$$y_m = 2\sqrt{\frac{\mu}{3(\delta + 2\delta^2)}} p_m = 4\sqrt{\frac{\mu}{3}} \omega = 2\sqrt{\delta + 2\delta^2}. \tag{39}$$

Figure 5(a) shows the numerically found limit cycle. Its amplitude is in a good agreement with the analytical estimate (39).

The approximation of the oscillation amplitude p_m can also be calculated using the balance equation of mechanical energy (19). For stationary motions we demand

$$0 = \frac{d}{dt}\langle H \rangle = \langle \dot{H} \rangle. \tag{40}$$

Hence for a limit cycle of period 2π on the plane $p_z = 0$ we get from (40)

$$0 = \frac{1}{2\pi} \int_0^{2\pi} d\theta \Gamma \left(\frac{p_y(\theta)}{2} \right) p_y(\theta), \tag{41}$$

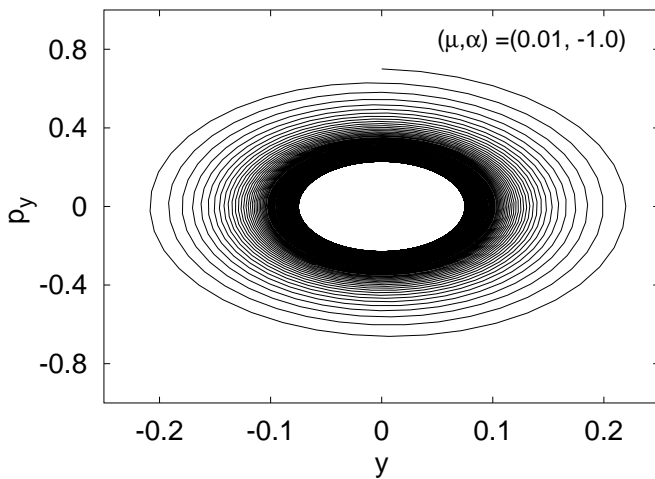
where θ is the angle coordinate. As shown above for small amplitudes of p_y (corresponding to small μ) we can replace the original Γ by the Rayleigh model. Using a harmonic oscillation ansatz for p_y we get the same oscillation amplitude p_m like in (39). The frequency ω given in (39) is the frequency of the linearization. Then automatically the y -amplitude is given by

$$y_m = \frac{p_m}{\omega}. \tag{42}$$

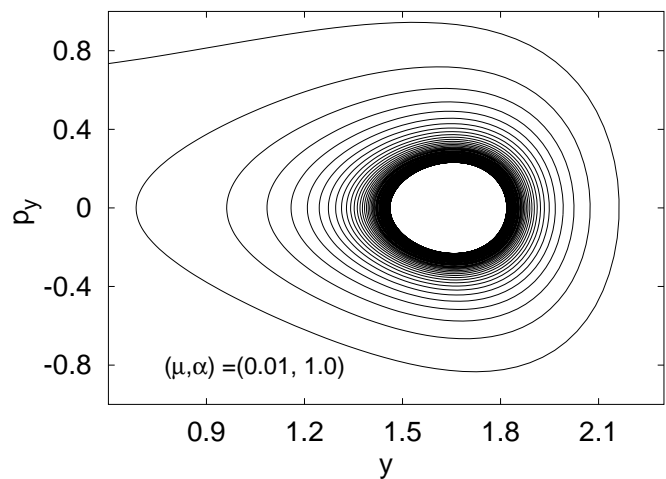
More generally Eq. (42) can be obtained by demanding that for periodic solutions the *Virial Theorem* holds. Neglecting center of mass motions we get from the theorem

$$2\langle K_y \rangle = \left\langle y \frac{\partial}{\partial y} U \right\rangle. \tag{43}$$

Here $K_y = p_y^2/2$ stands for the kinetic energy of the relative motion and $U = U(y)$ is explicitly given in (44). Both (40) and (43) together provide an algorithm to estimate the amplitudes of oscillations if the transformation (32) into the standard form



(a)



(b)

Fig. 5. Periodic orbit in the $(p_z = 0)$ -plane for the two particles Morse ring. (a) Mono-stable case, $\alpha < 0$. Initial conditions and parameter values are $(y(0), p_y(0), p_z(0)) = (0, 0.7, 0.3)$ and $\alpha = -1$ (this corresponds to $\delta = 0.86$). The amplitudes of the limit cycle are $y_m = 0.076$ and $p_m = 0.23$. Analytical estimate by (39) gives $y_m = 0.075$ and $p_m = 0.23$. (b) Bistable case, $\alpha > 0$. Initial conditions and parameter values are $(y(0), p_y(0), p_z(0)) = (0, 0.7, 0.3)$, and $\alpha = 1$ (this corresponds to $\delta = 0.32$). The second periodic orbit arises from reflection at the p_y -axis through $y = 0$. The amplitudes of the limit cycle are $y_m = 1.82$ and $p_m = 0.23$. Analytical estimate by (48) gives $(y - y_1)_m = 0.175$ with $y_1 = 1.66$ and $p_m = 0.23$.

(36) is not possible, but the structure of possible solutions is known.

Let us now consider $\alpha > 0$ when the interaction potential is also bistable. Similar to the previous situation we use $A = (1/2) - \delta$ with $\delta > 0$. Moreover we have $\delta < 1/2$ due to $A = 0.5e^{-\alpha} > 0$. The conservative contribution to the dynamics of the relative coordinate y in (32) is connected to the effective interaction potential

$$U(y) = 2A^2[\cosh(2y) - 1] - 4A[\cosh(y) - 1]. \quad (44)$$

The height of the potential wall between the minima $y_{1,2}$ existing for $\alpha > 0$ is $\Delta U = U(0) - U(y_{1/2}) = 4\delta^2$. Up to fourth order terms $U(y)$ can be approximated by the bistable potential

$$U(y) = \frac{\hat{a}}{2}y^2 + \frac{\hat{b}}{4}y^4 + \text{const.}, \quad (45)$$

known from the Duffing oscillator. The parameters are $\hat{a} = 4A(2A - 1)$ and $\hat{b} = (2/3)A(8A - 1)$. We begin our analysis with the case $\mu \ll \Delta U$. That means that the energy provided by the reservoir is not large enough to overcome the potential barrier. Thus we shall study the dynamics near the potential minima. Because of the U 's symmetry it is sufficient to investigate the dynamics near one of the steady states S_1 with $y = y_1$. Here the classical averaging method like in (36) still works. Introducing new coordinates $y = \beta u + y_1$, $p_y = \sqrt{\beta}v$, $p_z = \sqrt{\beta}w$ and $\tau = t/\sqrt{\beta}$ with $\beta = 8\delta(1 - \delta)$ and expanding we obtain from (32)

$$\dot{u} = v$$

$$\begin{aligned} \dot{v} = -u + \varepsilon \left\{ -6\sqrt{2}u^2 - \frac{\sqrt{2-2\delta}(3+16\delta-16\delta^2)}{24(\delta-1)^2\sqrt{\delta^3}}u^3 \right. \\ \left. -v[v^2+3w^2-32(1-\delta)\delta\mu] \right\} \\ \dot{w} = -\varepsilon w[3v^2+w^2-32(1-\delta)\delta\mu] \end{aligned} \quad (46)$$

with $\varepsilon = 1/64\sqrt{2\delta^3(1-\delta)^3}$. Averaging gives

$$\begin{aligned} \dot{a} &= -\varepsilon \frac{a}{8} \{3a^2 + 4[3w^2 - 32(1-\delta)\delta\mu]\} \\ \dot{w} &= -\varepsilon \frac{w}{2} \{3a^2 + 2[w^2 - 32(1-\delta)\delta\mu]\} \\ \dot{\phi} &= \varepsilon \frac{a^2\sqrt{2-2\delta}(3+16\delta-16\delta^2)}{64(\delta-1)^2\sqrt{\delta^3}}. \end{aligned} \quad (47)$$

From the stability analysis of the averaged system (47) we find for the original system (32) the stable

limit cycle with

$$\begin{aligned} (y - y_1)_m &= \sqrt{\frac{2\mu}{3(\delta - \delta^2)}} \quad p_m = 4\sqrt{\frac{\mu}{3}} \\ \omega &= 2\sqrt{2(\delta - \delta^2)} \end{aligned} \quad (48)$$

Comparing with (39) for the mono-stable case we have the same amplitude of momentum p_m but a different y -amplitude and frequency. This harmonic approximation requires $\mu \ll 2\sqrt{(2-2\delta)\delta}$. Because of the $y_{1,2}$ -symmetry we now have two limit cycles (one of them is plotted in [Fig. 5(b)]) in the ($p_z = 0$)-plane instead of the single limit cycle when $\alpha < 0$ [Fig. 5(a)]. All these limit cycles correspond to asymptotically stable anti-phase (optical) oscillations of the two particles on the ring. In the mono-stable case [Fig. 5(a)] the particles oscillate around the equilibrium distance $L/2$ ($\langle y \rangle = 0$), while in the bistable case [Fig. 5(b)] they oscillate within a cluster staying close to each other ($\langle y \rangle = 1.66$).

A further change in the attractor structure of the system (32) occurs, when the energy uptake rate q (respectively μ) is large enough to overcome the potential barrier ΔU , in other words when the pumping pushes the system over the separatrix existing only for positive α . In our computer experiments we realized this situation by changing ΔU and keeping μ constant. In this case the two limit cycles melt and the result is a single limit cycle which lies again in the invariant manifold (Fig. 6).

For an estimation of the new attractor the harmonic ansatz is not sufficient and we apply the solutions known from the conservative Duffing oscillator

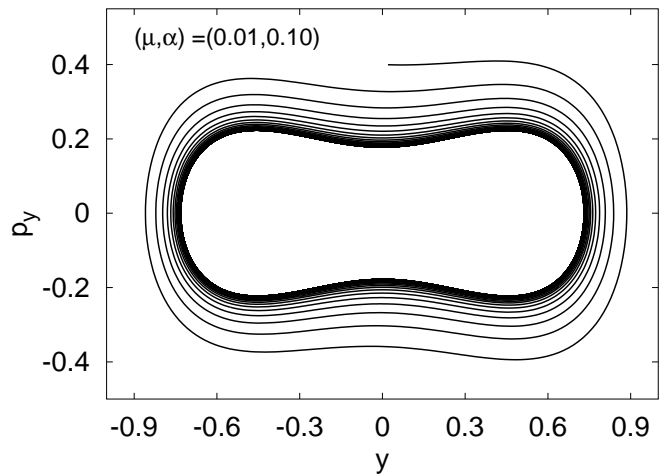


Fig. 6. Bistable Morse ring $N = 2$. Numerically calculated periodic orbit in the ($p_z = 0$)-plane with initial condition $(0, 0.4, 0)$.

(45) to the averaging concept generated by (40) and (43). This automatically implies that we restrict ourselves to low oscillation amplitudes i.e. small parameters μ and δ , because otherwise the deviation from the original system (32) will be too large. Actually we discuss at this point a Duffing system with Rayleigh pumping. Under these assumptions the equation for the homoclinic orbit connecting $(y, p_y) = (0, 0)$ to itself reads

$$p_y = \pm \sqrt{\hat{a}y^2 + \frac{\hat{b}}{2}y^4}. \tag{49}$$

For energy values $E > \hat{a}^2/4\hat{b}$ all solutions of the conservative Duffing problem are given by

$$y(t) = Y \operatorname{cn}(\theta, k) \quad \theta = \Omega t. \tag{50}$$

The oscillation frequency Ω is connected with the amplitude Y and the elliptic modulo $k \in (0, 1)$ by

$$\Omega = \sqrt{\hat{a} + \hat{b}Y^2} \quad k = \sqrt{\frac{\hat{b}}{2} \frac{Y}{\Omega}}. \tag{51}$$

The period of oscillations is $\Theta = 4\mathcal{K}(k)$ where $\mathcal{K}(k)$ is the complete elliptic integral of the first kind. A more detailed discussion of the Duffing system can be found in [Landa, 1996]. From (50) we get

$$\begin{aligned} p(t) &= Y\Omega \operatorname{sn}(\theta, k) \operatorname{dn}(\theta, k) \\ &= P \operatorname{sn}(\theta, k) \operatorname{dn}(\theta, k) \equiv P g(\theta, k). \end{aligned} \tag{52}$$

Using (40) and the Rayleigh-approximation we can calculate P (for $P \neq 0$) numerically for each value

k from the equation

$$P(k)^2 = 4\mu \frac{\int_0^{4\mathcal{K}(k)} d\theta g^2(\theta, k)}{\int_0^{4\mathcal{K}(k)} d\theta g^4(\theta, k)}. \tag{53}$$

For each pair $(P(k), k)$ we then calculate Y and Ω and test the criterion (43) by plotting the function

$$\Phi(k) = \langle \hat{a}y^2 \rangle + \langle \hat{b}y^4 \rangle - \langle p_y^2 \rangle. \tag{54}$$

with average values taken over period Θ . The value k^* satisfying $\Phi(k^*) = 0$ can be used to estimate the attractor amplitudes and frequencies. In the parameter region allowed by the approximation conditions the value k^* is unique. Figures 6 and 7(b) show the numerically calculated trajectory and its analytical estimation. The deviation of $\Delta Y = Y(k^*) - Y_{\text{num}}$ is slightly positive due to the neglected higher orders in the expansion of U .

We note that the method of the averaged elliptic functions is also very successful in the monostable region $\alpha < 0$. Here it is especially useful in the case of $\mu \geq \delta$ when the harmonic approximation is no longer satisfactory. In the bistable transition region $\alpha > 0$ and $\mu < 4\delta^2$ the method can also be applied using

$$y(t) = Y \operatorname{dn}(\Omega_1 t, k) \quad \Omega_1 = \sqrt{\frac{\hat{b}}{2}} Y \quad k = \frac{\Omega_1}{\Omega} \tag{55}$$

but the local expansion of the potential is no longer

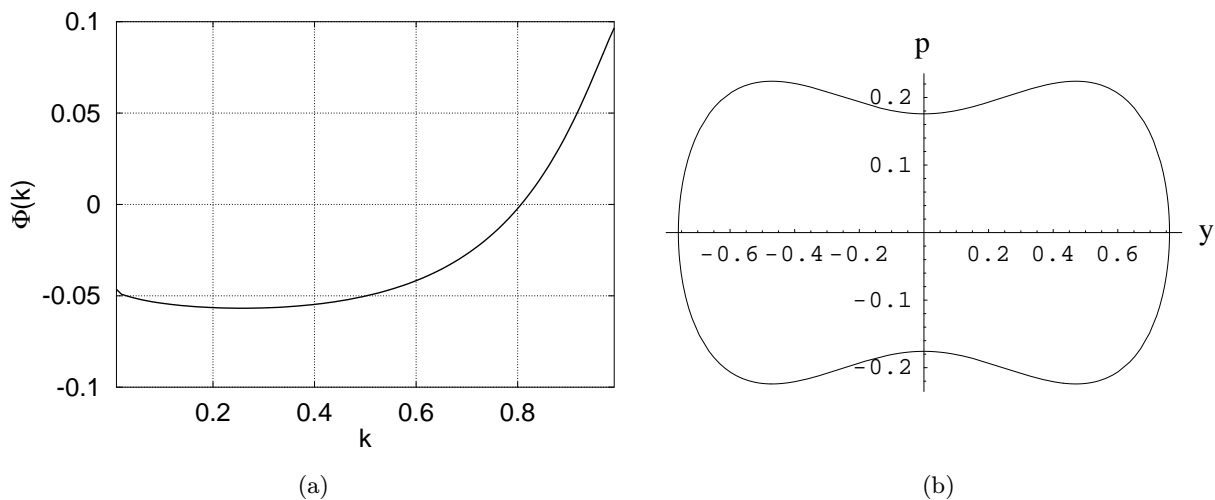


Fig. 7. Bistable Morse ring $N = 2$. (a) Plot of the test-function Φ . (b) Analytical approximation of the attractor by means of elliptical functions using $k^* = 0.805$. The parameters α, μ are the same like those in Fig. 6.

of Duffing type since the influence of cubic terms cannot be neglected. This fact leads to bigger deviations between approximation and numerically integrated limit cycles than in the other cases.

Due to the complicated structure of the phase space a statement concerning nonexistence of other attractors for (32) is difficult to prove. At this point we restrict ourselves to the results of extensive numerical experiments, which do not show any stable stationary motions other than the attractors described above. Finally, Fig. 8 summarizes the results of this section. The parameter space (α, μ) is divided by the bifurcation lines into five domains with qualitatively different dynamics in the phase space (y, p_y, p_z) . Region II corresponds to the globally stable steady state, S_0 , or to the rest state of the ring with equidistant particle distribution. When we pass from domain II into I, two bifurca-

tions occur at $\mu = 0$: (i) the steady state splits via a pitchfork bifurcation into three states. Two of them at $(0, 0, \pm\sqrt{\mu})$ are stable, (ii) steady state in the origin loses stability and a limit cycle is born via a Hopf bifurcation. Thus in the domain I depending on initial conditions three types of different motions can be realized: clockwise/counterclockwise rotations of the whole ring with equidistantly positioned particles or optical oscillations with mean particle distance $L/2$. Now if we cross the border between domains II and V the steady state in the origin, S_0 , splits into three new steady states. Two of them at $(\pm \cosh^{-1}[e^\alpha], 0, 0)$ are stable. They correspond to two cluster states, i.e. particles attract each other and spontaneously form a group. Then passing from domain V to IV a pitchfork and a Hopf bifurcations occur. In the domain IV we have six attractors. Two of them correspond to

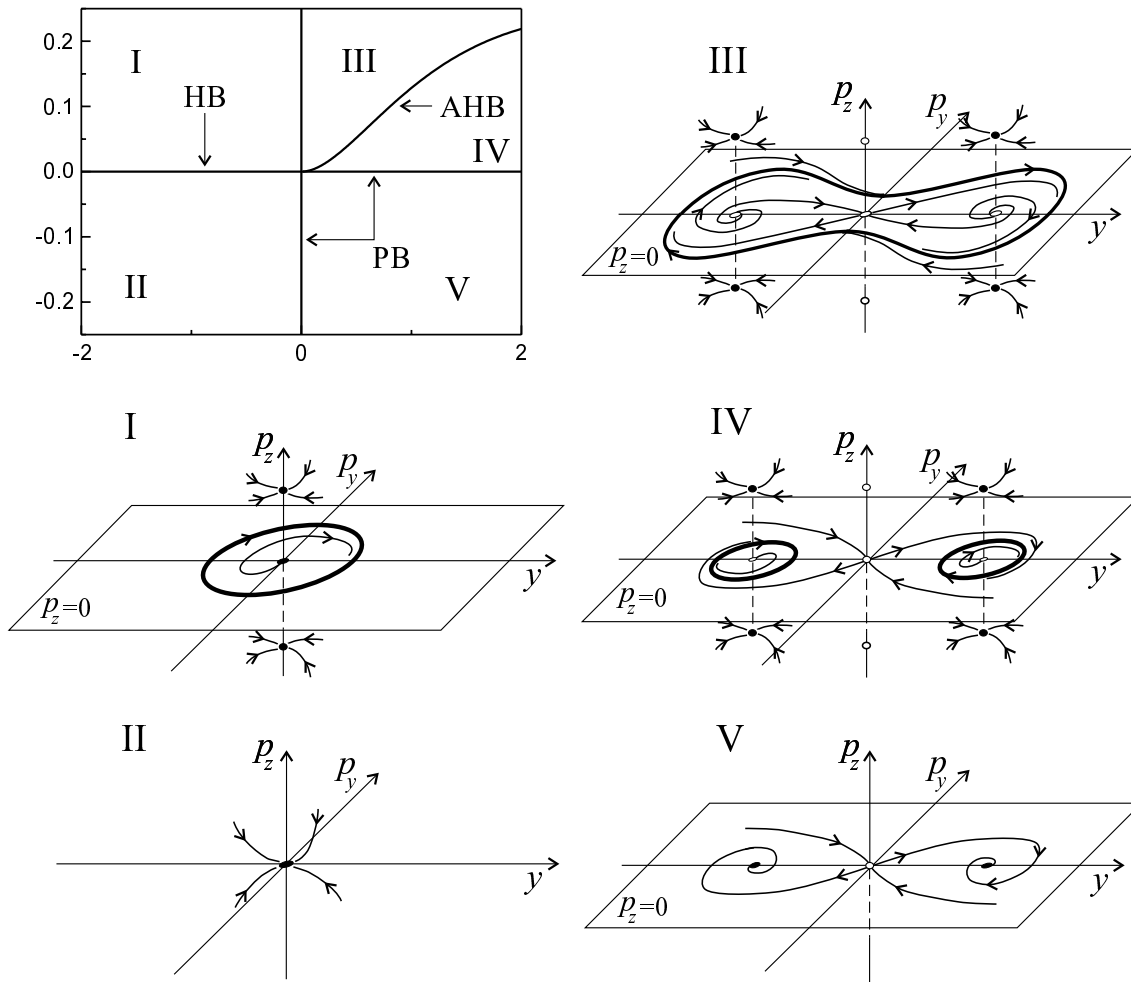


Fig. 8. Bifurcation diagram and sketches of the phase space for the different parameter regions. Abbreviations: PB for pitchfork bifurcation, HB for Hopf bifurcation and AHB for Andronov-homoclinic bifurcation. Stable/unstable steady states are marked by bold black/empty dots, respectively.

optical oscillations of the particles inside a cluster ($|\langle y \rangle| > 0$), while the others describe stationary clockwise/counterclockwise rotations of the particles grouped into cluster. Further, passing from domain IV to III an Andronov-homoclinic bifurcation occurs. Approaching the bifurcation the oscillation period diverges and an attracting homoclinic loop in $p_z = 0$ is formed. In domain III we have five attractors. Four of them (steady states) correspond to stationary rotations like in domain IV, but the limit cycle describe high amplitude oscillations of particles. Passing to domain I we observe pitchfork bifurcations of steady states and motions already described above.

4.2. Active Morse ring with $N > 2$

Having explicitly discussed the case of the smallest ring with $N = 2$ so far we will now extend our considerations to larger particle ensembles concentrating on qualitative effects. In Sec. 3 we have shown that there is a close relationship between Toda and Morse rings in the case of high densities. Therefore both interactions lead to the same types of attractors (uniform rotations with equal distances between the particles and $(N - 1)$ oscillatory modes) in this parameter region. These effects have been widely discussed in [Makarov *et al.*, 2001].

Hence we may now exclusively concentrate on the multistable case $n < \bar{n}_c$ corresponding to multistable potential energy U^M . But even for low den-

sities $n < \bar{n}_c$ an active Morse ring behaves qualitatively very similar to an active Toda ring as long as the pumping is very strong, i.e. $\mu \gg \Delta U^M = a/2b$. If this condition is satisfied the effects caused by the barriers in the effective potentials may be neglected and we may replace the effective interaction potentials in Fig. 2 by box-shaped cosh-potentials and obtain for such an approximation similar attractors like in a Toda ring. The $N - 1$ wave-like attractors again correspond to single and combinations of soliton-like waves and we also find uniform rotations. The only difference is that the rotations are not necessarily characterized by $r_i = l - \sigma$ anymore. The domain of qualitatively new effects is restricted to the parameter region of slightly overcritical pumping $0 < \mu \ll \Delta U^M$. Here we may generally say that all observed stationary motions are either uniform rotations with $\dot{s} = \pm\sqrt{\mu}$ or low amplitude stationary oscillations with $\dot{s} = 0$. If visiting a rotation attractor the system occupies a minimum of the potential energy, i.e. all motions of the relative coordinates r_i between the particles vanish. This statement is always true and can be easily proven by an ordinary stability analysis. In addition to the rotation attractors we find for $N > 2$ again further attractors corresponding to small (optical) oscillations around one of the minima of the potential energy. All oscillation attractors have in common that the “center of mass” coordinate comes to rest. For both rotation and oscillation attractors it only depends on the initial conditions for

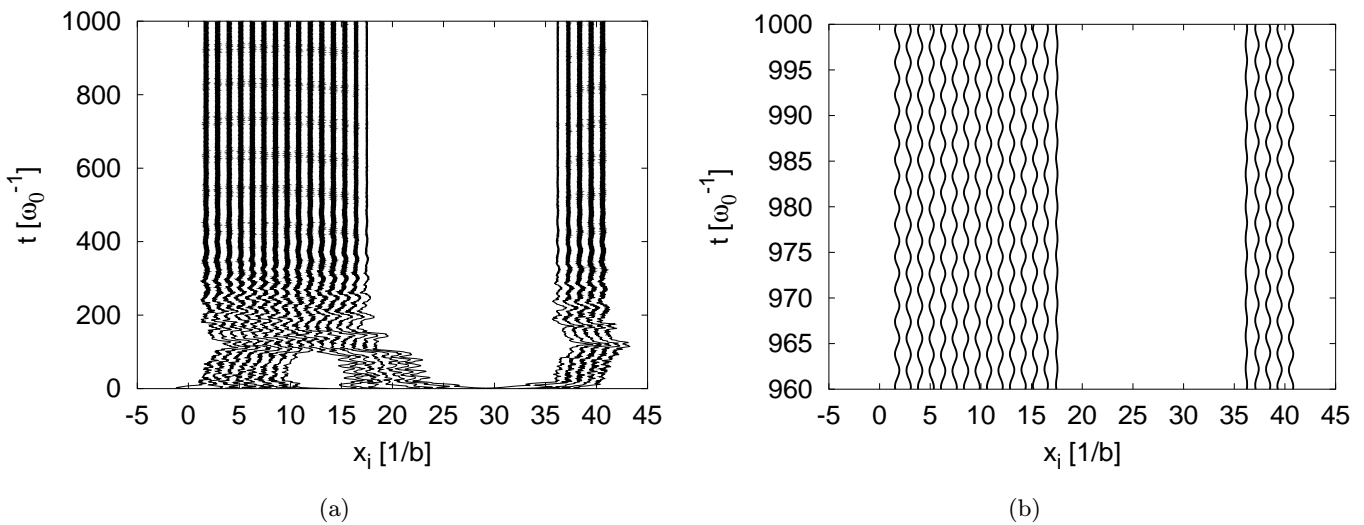


Fig. 9. Morse ring with $N = 20$ particles and subcritical particle density, $n < n_c$ (α, μ) = (0.307, 0.10). (a) Time evolution of the particle positions; (b) Enlarged part of (a) showing stationary optical oscillations inside a single big cluster.

which the minimum potential energy is visited. We remember that in the transition region $n \in (n_c, \bar{n}_c)$ the minima of the potential energy correspond either to $r_i = l - \sigma$ or single N -cluster configurations while for $n < n_c$ the cluster configurations remain as the only minima of U^M . In Fig. 9 we plot the stationary oscillations for a ring with $N = 20$ particles, low density $n < n_c$ and weak pumping $0 < \mu \ll \Delta U^M$. We emphasize that the last statements concerning a ring with many particles have to be understood as experimental results gained from extensive computer simulations with a big number of randomly chosen initial conditions.

5. Cluster Dynamics in a Dissipative, Noisy Morse Chain

In the previous sections we studied the deterministic $1d$ -Morse ring with regard to its attractor structure. We have seen that depending on the particle density, n , and the energy pumping constant, μ , there exists a large number of different stationary motions. Now we extend our investigations to the nondeterministic case by coupling the particles to a heat bath (e.g. liquid of smaller molecules). The interaction between the particles and the fluctuating bath is modeled by additive Gaussian white noise. Hence the full Langevin equations for our system now read as

$$\frac{dx_i}{dt} = v_i, \quad \frac{dv_i}{dt} - F_i = \Gamma(v_i) + \sqrt{2D}\zeta_i(t). \quad (56)$$

The case of purely passive friction ($\Gamma(v_i) = -\gamma_0 v_i$) corresponds to a thermodynamical equilibrium system. In this specific situation D , γ_0 and the physical temperature T of the heat bath are connected by the fluctuation-dissipation-theorem

$$D = \gamma_0 T. \quad (57)$$

Here we use an unit temperature $[T] = k_B^{-1}$ with k_B denoting the Boltzmann constant. The equilibrium theory of such systems corresponds to the statistical mechanics of a thermal $1d$ -gas and can be analyzed by well-known methods [Kac *et al.*, 1963; Feynman, 1972; Percus, 1987]. The equilibrium distribution function is known

$$f_N(r_1, \dots, r_N, v_1, \dots, v_N) \propto \exp\left[-\frac{H}{T}\right]. \quad (58)$$

For the nonequilibrium system characterized by a velocity-dependent friction function $\gamma(v^2)$ the quan-

tity $T = D/\gamma_0$ does not necessarily mean the physical temperature. For the time being we will consider T as an effective temperature converging to the physical temperature in the equilibrium limit $\gamma(v^2) \rightarrow \gamma_0$. Our aim is to study the density/noise-dependence of the cluster distributions for the $1d$ -Morse system described by (56) and to generate some sort of simple phase diagram. Therefore we integrate the stochastic equations (56) numerically using Euler algorithm and generate the mean stationary cluster distributions for different parameter constellations. In all computer experiments the noise sources $\zeta_i(t)$ are realized by random numbers taken from a standard normal distribution. According to our results from the previous sections clustering processes may only be observed in the case of low enough particle densities $n < \bar{n}_c$. More precisely, we shall limit our investigations on a ring with $n < n_c$ i.e. we also neglect the transition region $[n_c, \bar{n}_c]$ in our computer experiments at this point. Additionally, we fix the parameter value $\gamma_0 = 1$ thus a variation of μ is immediately connected to a variation of the energy uptake rate q . Since μ is the essential parameter for the deterministic pumping the fixing of γ_0 does not qualitatively affect the results. First we concentrate on the case of purely passive friction, which means $\mu = -1$ or $q = 0$. For the noise-free (deterministic) limit case, $D = 0$, we know from Sec. 3 that all motions come to rest after a finite relaxation time and all particles are situated in a single cluster of size N corresponding to a minimum of the potential energy of the ring. If we denote K as cluster size variable that can take values $k \in \{1, \dots, N\}$ the stationary cluster probability $P_D[K = k]$ in this situation is

$$P_0[K < N] = 0 \quad \text{and} \quad P_0[K = N] = 1. \quad (59)$$

In other words $P_D[K = k]$ is the probability of finding a cluster of size k on the ring at time $t \rightarrow \infty$. If we increase the noise intensity, $D > 0$, probability flows from the value $k = N$ to values $k < N$. We calculate $P_{D>0}[K = k]$ numerically from the relative frequency of finding a cluster of size k during several measurements over time intervals $\Delta t = t_2 - t_1$ with $t_2 > t_1 \gg 0$. Figures 10(a) and 10(b) show the numerically determined probabilities averaged over the time interval $t \in [800, 1000]$ for different values of D in a ring with five particles. To distinguish cluster states we demand that the distance between two particles has to be smaller than 1.7. Figure 10(a) corresponds to the equilibrium situation ($q = 0$, $\mu = -1$) and Fig. 10(b) to the case

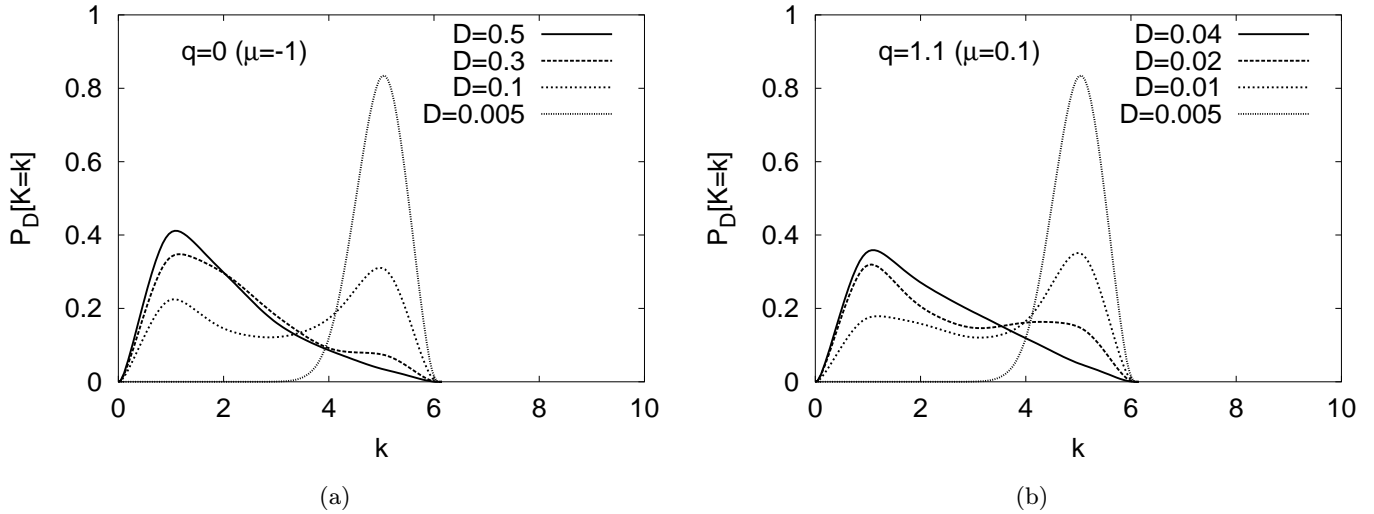


Fig. 10. Probability of cluster configurations in a multistable Morse ring ($N = 5$) in the presence of Gaussian white noise ($\sigma = 1$, $\gamma_0 = 1$, $\Delta U^M = 0.5$ and $\alpha = 0.807$ corresponding to mean particle density $n = 0.4 < n_c = 0.59$). (a) Purely passive friction ($q = 0$). The clusters disappear as soon as the thermal energy (effective temperature) becomes higher than the depth ΔU^M of the Morse potential. (b) For the nonequilibrium system the distribution functions are qualitatively similar but the critical effective temperature $T_c = D_c/\gamma_0$ is much lower than ΔU^M .

of over-critical pumping ($q = 1.1$, $\mu = 0.1$). Both diagrams show qualitatively the same behavior. For small D (or T , respectively) the particles are most likely gathered together in one big cluster. Increasing the strength of noise the big clusters split into smaller ones and the shape of the probability distribution changes. We can say the system visits the metastable states explained in Sec. 3 corresponding to a mixture of smaller clusters (monomers, dimers, etc). For a certain critical value of noise intensity, D_c , the distribution function has a single maximum at $K = 1$. This means that there are no clusters anymore. In the equilibrium situation [Fig. 10(a)] the corresponding critical temperature $T_c = D_c/\gamma_0$ has to be of the same order like the depth of the Morse potential $\Delta U^M = U_i^M(0)$ and we obtain from (3) and (15)

$$T_c \approx \Delta U^M = \frac{a}{2b} = \frac{1}{2}. \quad (60)$$

The numerically found value $T_c \approx 0.4$ confirms this assumption. In the case of over-critical pumping $\mu > 0$ the clusters completely disappear at low temperature values $T_c \approx 0.04$. In both equilibrium and nonequilibrium situations this change in the stationary cluster distributions might be interpreted as a “smooth phase transition” of van-der-Waals type. The additional energy input for $q > \gamma_0$ from the reservoir helps the particles to overcome the binding energy faster than in the case of $q = 0$ and the big clusters decay already for lower effective

temperatures T into smaller ones. This explains the decrease of the critical temperature T_c . It is clear that in principle clustering processes may not be observed if $\mu \gg a/b$ because then the deterministic energy supply from the external reservoir already prevents the formation of clusters. Figure 11 shows the traces of the particles for a Morse ring with $N = 20$ particles in the presence of noise. Clusters are dynamically split and recreated. We may say that for high particle densities $n > \bar{n}_c$ the model behaves similar to an $1d$ -solid body because then it is similar to a Toda chain. In the transition region $\bar{n}_c > n > n_c$ the system can dynamically switch between clustering and nonclustering states. But this is only observable for low enough effective temperatures, T , and weak pumping. If we decrease the density such that $n < n_c$ the particles can assemble in clusters as long as $T < T_c$. This bears some analogy to the formation of liquid-like states. At high temperatures, $T > T_c$, and low particle densities, $n < n_c$, the stochastic forces dominate the dynamics, the clusters are completely destroyed and we can imagine the model to represent a $1d$ -gas. On this basis we develop a simple diagram qualitatively illustrating the clustering effects with respect to the particle density, n , and the effective temperature T (Fig. 12). A more quantitative analysis of the clustering phenomena is a nontrivial problem due to the combination of the nonlinear deterministic energy input and the stochastic (thermal) effects

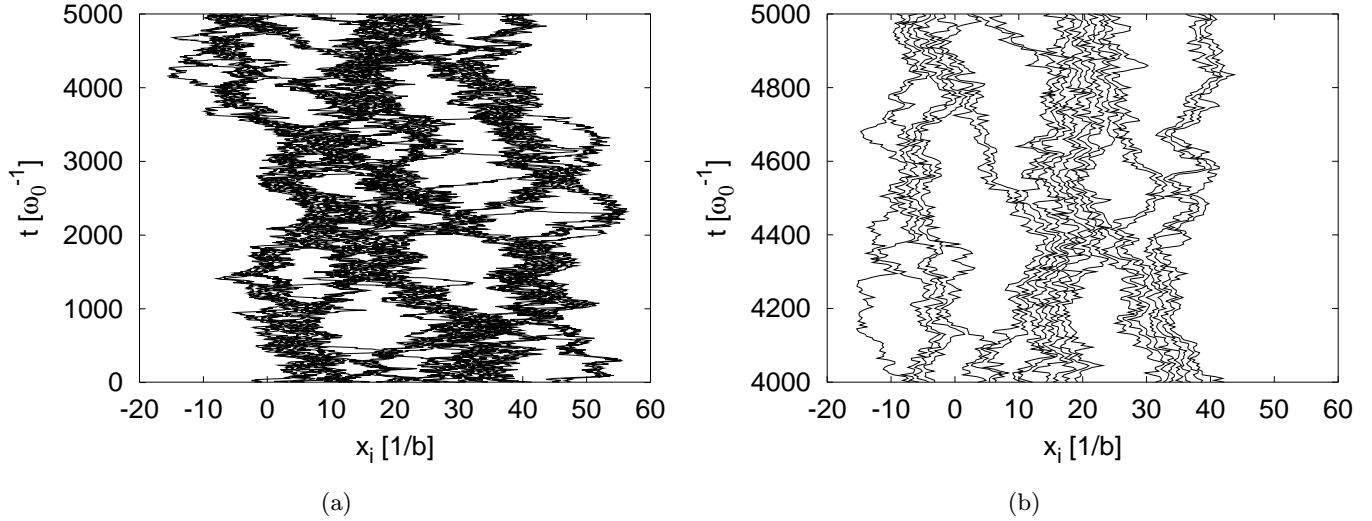


Fig. 11. Multistable Morse ring with $N = 20$ particles in the presence of white noise ($D = 0.1$). The diagrams show the paths $x_i(t)$ for each Brownian particle in the case of purely passive friction ($\mu = -1$). The other parameters are $n = 0.4 < n_c = 0.59$, $\gamma_0 = 1$ and $\sigma = 1$. One can see decay and formation of clusters. The pictures for the nonequilibrium system $\mu > 0$ look qualitatively similar as long as $(\mu/2) + T \ll \Delta U^M$.

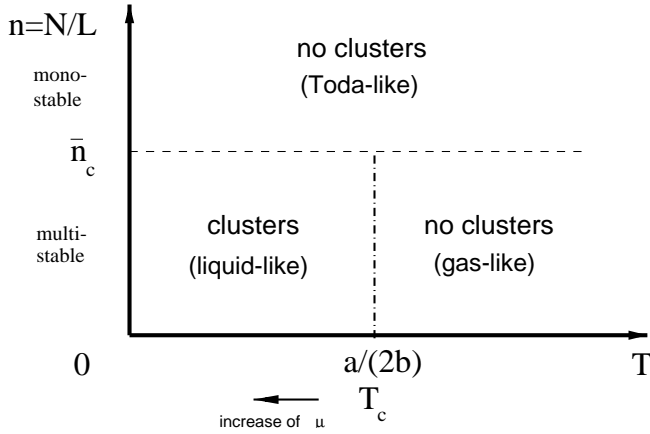


Fig. 12. Schematic phase transition-like diagram. The dashed-dotted line indicates the transition temperature for the equilibrium system corresponding to $\mu = -1$. For increasing μ the (T, n) -region featuring clusters becomes smaller, i.e. $T_c \ll \Delta U^M = a/(2b)$. If $\mu/2 \gg \Delta U^M$ we have $T_c = 0$, i.e. clusters do not exist anymore.

in this model and we leave this question for the future.

6. Conclusions

As an 1d-model of dissipative nonlinear rings we have studied a homogeneous Morse ring consisting of N active Brownian particles. In contrast to Toda rings which have been investigated in earlier works we have shown that the dynamics of the Morse ring strongly depends on the mean particle density $n = N/L$. For a Morse ring there exists a critical

density n_c such that for low densities $n < n_c$ the potential energy has N equivalent minima corresponding to the case when all particles attend to a single cluster. Additionally there exists a second critical value of particle density $\bar{n}_c \geq n_c$ such that there is only one single minimum of the potential energy if $n > \bar{n}_c$ which corresponds to an equidistant distribution of the particles on the ring. In the transition region $\bar{n}_c > n > n_c$ both clustering and nonclustering effects may be observed. For very high densities $n \gg \bar{n}_c$ a conservative Morse ring with stiffness parameter b asymptotically behaves like a Toda ring with stiffness parameter $2b$. This also remains true if we add deterministic and stochastic dissipative terms to the motion equations. Thus in the limit of high densities all previously known results from dissipative Toda systems [Bolterauer & Opper, 1981; Makarov *et al.*, 2001; Ebeling *et al.*, 2000] may be applied as well to a Morse ring. Using a friction function derived from a depot model [Schweitzer *et al.*, 1998; Ebeling *et al.*, 1999] we have shown that over-critical deterministic pumping in a Morse ring leads to different types of stationary motions corresponding to certain attractors (steady states and periodic orbits) in the phase space. For high particle densities $n > \bar{n}_c$ we find for a Morse ring with N particles $N+1$ attractors which can be identified as the stable uniform rotations (with equal distances $1/n$ between the particles and mean velocities $\pm\sqrt{\mu}$), soliton-like waves, etc. are already observed in a Toda ring. New effects occur if the

particle density is lower than the second critical value, $n < \bar{n}_c$. Now the rotation attractors can also correspond to rotating clusters of size N . For $n < n_c$ all stationary rotations are cluster rotations. With regard to more complicated attractors we have to distinguish between situations where the energy provided by the nonlinear friction is higher or lower than the binding energy approximately given by the depth of the Morse potential ΔU^M . In the first case of strong pumping $\mu \gg \Delta U^M$ the attractor structure is again similar to that of a Toda ring. This is because the pumping pushes the system to a mean energy level where the exponentially repulsive forces dominate. Hence we find again $N - 1$ oscillatory modes familiar from the studies of Toda models. For the remaining situation of over-critical but weak pumping $0 < \mu \ll \Delta U^M$ the only attractors found in addition to the cluster rotations are given by small oscillations of the particles around the minima of the full potential energy U^M . On the oscillation attractors the “center of mass” coordinate comes to rest. In case of even particle numbers we have optical anti-phase oscillations, otherwise the phase relations are more complicated. Most of the main characteristics of the Morse ring are already observable for the first nontrivial case with two particles that we have been able to treat analytically.

Because of the 1d-effects observed in this model an extension to higher dimensions seems to be interesting. This could happen with regard to complex motions of active clusters e.g. rotations of two- or three-dimensional clusters. On the other hand one could also think of an extension of the one-dimensional model, e.g. with respect to additional external force fields it could be used as a physical approach to investigate traffic (e.g. jams) or transport phenomena. But first of all we intend to continue investigations of the noisy 1d-model in order to obtain a deeper understanding of its nonequilibrium behavior which has been discussed with regard to cluster distributions here. In this sense the work represented in this paper should also be considered as a basis for subsequent investigations of transitions in a nonequilibrium Morse system.

Acknowledgments

The authors are grateful to M. G. Velarde and L. Schimansky-Geier for support of this work and for many helpful discussions. This work was fi-

nancially supported by the DFG via the Sfb555 (J. Dunkel and U. Erdmann) and by the Humboldt-Mutis Foundation (W. Ebeling). V. A. Makarov benefited from the support provided by the Spanish Ministry of Science and Technology.

References

- Bolterauer, H. & Opper, M. [1981] “Solitons in the statistical mechanics of the Toda lattice,” *Z. Phys.* **B42**, 155–161.
- Christov, C. I. & Velarde, M. G. [1995] “Dissipative solitons,” *Physica* **D86**, 323–347.
- Chu, X. L. & Velarde, M. G. [1991] “Korteweg–de Vries soliton excitation in Benard–Marangoni convection,” *Phys. Rev.* **A43**, 1094–1096.
- Ebeling, W., Jenssen, M. & Romanowsky, Y. M. [1989] “Irreversible processes and selforganization,” *Teubner Texte Physik*, Vol. 23 (Teubner Leipzig), pp. 7–24.
- Ebeling, W. & Jenssen, M. [1991] “Soliton-assisted activation processes,” *Ber. Bunsenges. Phys. Chem.* **95**, 1356–1362.
- Ebeling, W., Schweitzer, F. & Tilch, B. [1999] “Active Brownian particles with energy depots modelling animal mobility,” *BioSyst.* **49**, 17–29.
- Ebeling, W., Erdmann, U., Dunkel, J. & Jenssen, M. [2000] “Nonlinear dynamics and fluctuations of dissipative Toda chains,” *J. Stat. Phys.* **101**, 443–457.
- Erdmann, U., Ebeling, W., Schimansky-Geier, L. & Schweitzer, F. [2000] “Brownian particles far from equilibrium,” *Eur. Phys. J.* **B15**, 105–113.
- Feynman, R. P. [1972] *Statistical Mechanics* (Benjamin Mass.).
- Guckenheimer, J. & Holmes, P. [1983] *Nonlinear Oscillations, Dynamical Systems, and Bifurcations of Vector Fields*, Vol. 42 (Springer).
- Jenssen, M. & Ebeling, W. [2000] “Distribution functions and excitation spectra of Toda systems at intermediate temperatures,” *Physica* **D141**, 117–132.
- Kac, M., Uhlenbeck, G. E. & Hemmer, P. C. [1963] “On the van der Waals theory of the vapor–liquid equilibrium,” *J. Math. Phys.* **4**, 216–228.
- Landa, P. [1996] *Nonlinear Oscillations and Waves in Dynamical Systems* (Kluwer Academic Publishers, Dordrecht).
- Makarov, V., Ebeling, W. & Velarde, M. [2000] “Soliton-like waves on dissipative Toda lattices,” *Int. J. Bifurcation and Chaos* **10**, 1075–1089.
- Makarov, V. A., del Rio, E., Ebeling, W. & Velarde, M. G. [2001] “Dissipative Toda-Rayleigh lattice and its oscillatory modes,” *Phys. Rev.* **E64**, 036601.
- Percus, J. K. [1987] “Exactly solvable models of classical many-body systems,” *Studies in Statist. Mech.* **13**, 1–158.
- Rayleigh, J. W. [1945] *The Theory of Sound*, Vol. 1, 2nd edition (Dover, NY).

Schweitzer, F., Ebeling, W. & Tilch, B. [1998] "Complex motion of Brownian particles with energy depots," *Phys. Rev. Lett.* **80**(23), 5044–5047.

Toda, M. [1983] *Nonlinear Waves and Solitons* (Kluwer Academic Publishing, Dordrecht).

Toda, M. & Saitoh, N. [1983] "The classical specific heat of the exponential lattice," *J. Phys. Soc. Japan* **52**, 3703–3705.

Wiggins, S. [1996] *Introduction to Applied Nonlinear Dynamical Systems and Chaos* (Springer, Dordrecht).